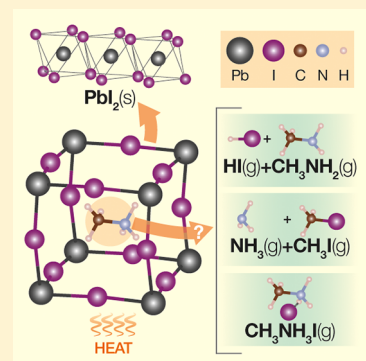


# 1 Thermodynamics and the Intrinsic Stability of Lead Halide 2 Perovskites $\text{CH}_3\text{NH}_3\text{PbX}_3$

3 Andrea Ciccioli\*<sup>1</sup> and Alessandro Latini<sup>2</sup>

4 Department of Chemistry, Sapienza – University of Rome, Piazzale Aldo Moro 5, 00185 Rome, Italy

5 **ABSTRACT:** The role of thermodynamics in assessing the intrinsic instability of the  
6  $\text{CH}_3\text{NH}_3\text{PbX}_3$  perovskites ( $X = \text{Cl}, \text{Br}, \text{I}$ ) is outlined on the basis of the available  
7 experimental information. Possible decomposition/degradation pathways driven by the  
8 inherent instability of the material are considered. The decomposition to precursors  
9  $\text{CH}_3\text{NH}_3\text{X}(\text{s})$  and  $\text{PbX}_2(\text{s})$  is first analyzed, pointing out the importance of both the  
10 enthalpic and the entropic factor, the latter playing a stabilizing role making the stability  
11 higher than often asserted. For  $\text{CH}_3\text{NH}_3\text{PbI}_3$ , the disagreement between the available  
12 calorimetric results makes the stability prediction uncertain. Subsequently, the gas-  
13 releasing decomposition paths are discussed, with emphasis on the discrepant results  
14 presently available, probably reflecting the predominance of thermodynamic or kinetic  
15 control. The competition between the formation of  $\text{NH}_3(\text{g}) + \text{CH}_3\text{X}(\text{g})$ ,  $\text{CH}_3\text{NH}_2(\text{g}) +$   
16  $\text{HX}(\text{g})$  or  $\text{CH}_3\text{NH}_3\text{X}(\text{g})$  is analyzed, in comparison with the thermal decomposition of  
17 methylammonium halides. In view of the scarce and inconclusive thermodynamic studies  
18 to-date available, the need for further experimental data is emphasized.



19 It is no exaggeration to say that the largest part of the current  
20 research efforts on lead halide-based and similar perovskite  
21 materials is directed toward the search for higher stability  
22 needed in photovoltaic applications. In the last five years, many  
23 authors expressed the concern that the low stability under the  
24 action of a number of external agents, including other device  
25 components, could be the main Achilles' heel of this class of  
26 light harvester materials, very attractive in other respects,  
27 whose prototype is the well-known methylammonium lead  
28 iodide,  $\text{CH}_3\text{NH}_3\text{PbI}_3$ .<sup>1–6</sup> As a consequence, a wealth of  
29 strategies were put in place to improve the material and  
30 device stability, based on chemical modifications<sup>7–9</sup> protection  
31 layers,<sup>10</sup> and encapsulation.<sup>11</sup>

32 Interaction with water/moisture has been soon identified as  
33 a major drawback.<sup>12</sup> Other external agents which many  
34 researchers focused on are oxygen and UV/visible radiation.<sup>13</sup>  
35 The study of these degradation processes was typically  
36 performed by following the change of properties/performances  
37 of the material/device, while the interaction takes place or *ex*  
38 *post*. To elucidate the progress and mechanism of degradation,  
39 a “microscopic” approach is most often applied, based on  
40 techniques such as XRD, UV–vis and NIR spectroscopy,  
41 fluorescence, microscopy, XPS, etc.<sup>14–17</sup> Theoretical calcu-  
42 lations may be of help in identifying mechanistic details.<sup>18</sup> The  
43 effect of temperature on the perovskite stability was usually  
44 studied in conjunction with that of such chemical and physical  
45 agents. Incidentally, it should be mentioned that in some cases  
46 the diagnostic means used to study degradation (e.g., X-ray  
47 irradiation, electron currents) can themselves play a role in  
48 degradation phenomena.<sup>19,20</sup>

49 Comparatively little work has been carried out on the  
50 intrinsic (in)stability of these materials in itself, both *in vacuo*  
51 and under inert atmosphere, as a function of temperature.<sup>21–24</sup>

In particular, very few studies are available based on a 52  
macroscopic thermodynamic approach.<sup>25–27</sup> Moreover, the 53  
available experimental and computational results are often 54  
discrepant. The goal of this Perspective is to discuss the issue 55  
of the intrinsic stability of  $\text{CH}_3\text{NH}_3\text{PbX}_3$  materials from a 56  
thermodynamic point of view in light of the information 57  
currently available, pointing out the persistent uncertainties 58  
and inconsistencies, which make urgent further experimental 59  
efforts. Special focus is done on the decomposition processes 60  
leading to the release of gaseous products. 61

Overall, we would like to emphasize in this paper the 62  
contribution that classic macroscopic thermodynamics can (or 63  
cannot) provide to the stability issues raised from the 64  
application of these materials to energy conversion technolo- 65  
gies. It is important to underline that the thermodynamic 66  
characterization of a material as such is a crucial prerequisite to 67  
undertake reliable thermodynamic predictions and simulations 68  
of its behavior in various chemical and physical environments. 69  
Furthermore, ascertaining the intrinsic (in)stability of a 70  
material is essential for practical applications, because if the 71  
material is found to be inherently unstable, any protection 72  
strategy may be undermined. Regrettably, from an analysis of 73  
the literature trends, one has the clear impression that 74  
experimental thermodynamic studies cannot keep pace with 75  
the wealth of new material modifications that are proposed at 76  
an ever-increasing rate to overcome instability issues. 77 p

In the broadest sense, investigating the thermodynamic 78  
stability of a material means to wonder if, under a given set of 79  
external conditions, the material will remain unchanged or it 80

Received: February 12, 2018

Accepted: June 14, 2018

Published: June 14, 2018

Ascertaining the intrinsic (in)-stability of a material is essential for practical applications, because if the material is found to be inherently unstable, any protection strategy may be undermined.

will undergo some kind of chemical/physical transformation, ultimately driven by entropy production. The number of possible transformation pathways of the system is, in general, high and difficult to predict. In a stricter and more practical sense, one usually evaluates the thermodynamic driving force or affinity,  $\Delta_r G = \sum_i \nu_i \mu_i$ , for one or a few among the many possible decomposition/degradation reactions, where  $\nu_i$  and  $\mu_i$  are, respectively, the stoichiometric coefficients (taken as negative for the left-hand reactants of the chemical/physical degradation process) and the chemical potentials of all the species involved. If the affinity is found to be negative under the conditions of interest (for example, for given pressure and temperature), the selected decomposition/degradation path is thermodynamically favored. Otherwise, the material is stable as far as that path is considered, and indeed its formation from right-hand products is thermodynamically favored. In this approach, the final products of the process are to be known or an hypothesis has to be done. In the case of  $\text{CH}_3\text{NH}_3\text{PbX}_3$  compounds, the decomposition to the synthesis precursors was most often considered in theoretical evaluations (Figure 1):

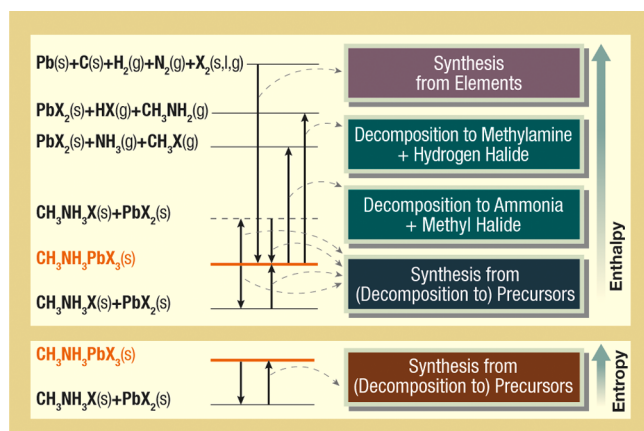
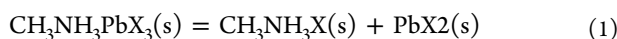


**Figure 1.** Enthalpy and entropy level scheme for possible formation/decomposition processes of  $\text{CH}_3\text{NH}_3\text{PbX}_3$  perovskites. Decomposition to precursors can be both endothermic and exothermic. The minor process leading to the formation of  $\text{CH}_3\text{NH}_3\text{X}(\text{g})$  (see Figure 3) is not shown. Enthalpy levels are not to scale.

Although considering this reaction is probably the most natural choice in assessing the formability of  $\text{CH}_3\text{NH}_3\text{PbX}_3$  compounds, it should be noted that, while  $\text{PbI}_2(\text{s})$  was much often reported as the main decomposition product under various conditions, apparently no experimental study reported the  $\text{CH}_3\text{NH}_3\text{X}$  solids among the observed products.

A huge number of theoretical calculations were performed to evaluate the energy/enthalpy change of the above reaction by

the DFT approach. However, the results are significantly dependent on the chosen functional, the best performance being usually obtained with the PBEsol one, with the additional inclusion of spin-orbit contributions.<sup>28,29</sup> A fairly rich selection of results is reported in Table 1. As for experiments, regrettably, only two direct determinations of  $\Delta_r H^\circ(1)$  are available in the literature, both obtained by solution calorimetry at  $T = 298 \text{ K}$ , using  $\text{DMSO}$ <sup>25</sup> or aqueous  $\text{HCl}$ <sup>26</sup> as a solvent. Note that, although at  $298 \text{ K}$   $\text{CH}_3\text{NH}_3\text{PbI}_3$  is stable in the tetragonal form, measurements of ref 25 were performed on the (metastable) cubic high temperature phase. A third experimental value for reaction 1 can be derived from the vapor pressure measurements carried out by effusion-based techniques on the equilibrium (reaction 8) discussed in the next section.<sup>27</sup>

A compilation of all the results is reported in Table 1. Somehow surprisingly, the two calorimetric determinations are not in agreement, showing a discrepancy definitely outside the claimed experimental uncertainties. For  $\text{CH}_3\text{NH}_3\text{PbI}_3$ , in particular, the very negative value of  $\Delta_r H^\circ(1)$  found in ref 26, which led those authors to claim the instability of the compound, was not confirmed by the subsequent measurements in  $\text{DMSO}$ ,<sup>25</sup> making difficult any conclusive prediction on the spontaneous direction of reaction (1) at room temperature for  $X = \text{I}$ . Also the stability trend from  $\text{Cl}$  to  $\text{Br}$  to  $\text{I}$  is not in agreement between the two studies (Figure 2). The values of ref 26 suggest the  $\text{Cl} > \text{Br} > \text{I}$  stability trend, which is consistent with the Goldschmidt's tolerance factor traditionally used to rationalize the stability of perovskite phases. However, tensimetric results<sup>27</sup> agree well with the Ivanov's data,<sup>25</sup> which is a nice occurrence in view of the completely different experimental approach used.

While the enthalpic term is often the most important factor driving the thermodynamic direction of an isothermal chemical

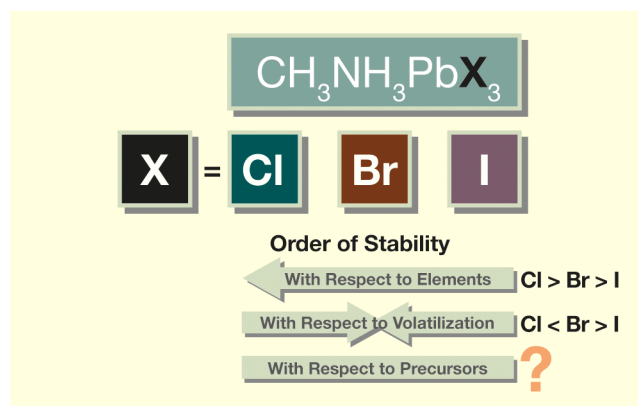
While the enthalpic term is often the most important factor driving the thermodynamic direction of an isothermal chemical reaction, it may well be that the entropic factor comes into play and affects the spontaneity evolution in a decisive manner.

reaction, it may well be that the entropic factor comes into play and affects the spontaneity evolution in a decisive manner. This is especially true for reactions involving gaseous phases, aggregation/disaggregation processes, high temperatures, and when enthalpic effects are small, which is the case of reactions (1). Regrettably, in the last few decades the number of papers presenting heat capacity and absolute entropy measurements is decreasing, making thermodynamic evaluations more difficult and less accurate. It is thus a really lucky occurrence that almost 30 years ago, when lead halide perovskites were far from bursting on the scientific scene, Suga and co-workers published low temperature heat capacity data for the  $\text{CH}_3\text{NH}_3\text{PbX}_3$  crystal phases.<sup>41</sup> Absolute entropies of the other compounds involved in reaction 1 are known with the exception of  $\text{CH}_3\text{NH}_3\text{Br}$ , whose entropy was estimated by us by the empirical Volume-Based-Thermodynamic approach.<sup>42</sup>

**Table 1. Energetic and Thermodynamic Properties of the Decomposition Reactions of  $\text{CH}_3\text{NH}_3\text{PbX}_3$  Perovskites to Solid Precursors:  $\text{CH}_3\text{NH}_3\text{PbX}_3(\text{s}) = \text{CH}_3\text{NH}_3\text{X}(\text{s}) + \text{PbX}_2(\text{s})^a$** 

X	theory (DFT)		thermodynamic experiments					
	$\Delta E^b$	ref.	$\Delta H_{298\text{K}}^\circ$	method and ref	$S_{298\text{K}}^\circ$ <sup>c</sup>	$\Delta S_{298\text{K}}^\circ$ <sup>d</sup>	$\Delta G_{298\text{K}}^\circ$	stable with respect to precursors at 298 K, 1 bar <sup>e</sup>
Cl (cubic)	12	30	$9.03 \pm 1.68$	solution calorim. in HCl <sup>26</sup>	313.37	-38.77	11.6	YES
	68	31	$4.45 \pm 0.34$	solution calorim. in DMSO <sup>25</sup>			16.0	YES
	0.39–3.9	32	$2.8 \pm 7.8$	vapor pressure (KEML, KEMS) <sup>27</sup>			11.6	YES
Br (cubic)	12	30	$-6.69 \pm 1.41$	solution calorim. in HCl <sup>26</sup>	349.29	-39.9	5.2	YES
	24	31	$6.78 \pm 0.97$	solution calorim. in DMSO <sup>25</sup>			18.7	YES
	1.4–4.1	32	$3.3 \pm 8.7$	vapor pressure (KEML, KEMS) <sup>27</sup>			15.2	YES
I (tetragonal)	2.7–3.4	22		solution calorim. in HCl <sup>26</sup>	374.15	-39.6	-22.7	NO
	9.6	33	$-34.50 \pm 1.01$					
	2.2	29						
	4.8	34						
	-8.7	35	$-1.913 \pm 1.12^f$	solution calorim. in DMSO <sup>25</sup>			9.9	YES
	5.8	36						
	9.6	31						
	-5.8/-6.1	32						
I (cubic) <sup>g</sup>	0.39	37	$0.39 \pm 9.7$	vapor pressure (KEML, KEMS) <sup>27</sup>			11.4	YES
	2.4	38						
	3.9	39						
	-4.8	28	$-4.493 \pm 1.12$	solution calorim. in DMSO <sup>25</sup>	383.85 <sup>c</sup>	-49.3	10.2	YES
	-1.9	30						
	26	40						
	-11/-12	32						

<sup>a</sup>Energies and enthalpies are in kJ/mol, entropies in J/K mol. <sup>b</sup>For an accurate comparison of the theoretical  $\Delta E$ s with the thermochemical  $\Delta H_{298\text{K}}^\circ$ , small effects due to zero-point energy, finite temperature and standard pressure should be considered. The corrections due to the heat content difference ( $H_{298\text{K}} - H_{0\text{K}}$ ) and the  $P^\circ\Delta V$  terms are of the order of few kJ/mol and J/mol, respectively. <sup>c</sup>Absolute entropies of  $\text{CH}_3\text{NH}_3\text{PbX}_3$  are from ref 41. The value for the high temperature cubic phase of  $\text{CH}_3\text{NH}_3\text{PbI}_3$  was estimated by adding the tetragonal-cubic transition entropy (9.7 J/K mol, measured at 330 K<sup>41</sup>) to  $S_{298\text{K}}^\circ$  of the tetragonal phase. <sup>d</sup>Entropies of  $\text{CH}_3\text{NH}_3\text{X}(\text{s})$  and  $\text{PbX}_2(\text{s})$  are from the compilation of ref 25, except for  $\text{CH}_3\text{NH}_3\text{Br}$ , whose  $S_{298\text{K}}^\circ$  was estimated by us as 148.2 J/K mol by a volume-based-thermodynamics approach.<sup>42</sup> <sup>e</sup>Based on the sign of  $\Delta G_{298\text{K}}^\circ$ , which for reactions (1) corresponds to the driving force  $\Delta_r G$  at 298 K and 1 bar. <sup>f</sup>Evaluated by adding the t-c transition enthalpy (2.58 kJ/mol, measured at 330 K<sup>41</sup>) to the  $\Delta H_{298\text{K}}^\circ$  value measured for the cubic phase. <sup>g</sup>The tetragonal to cubic transition enthalpy of  $\text{CH}_3\text{NH}_3\text{PbI}_3$  is 2.58 kJ/mol, measured at 330 K.<sup>41</sup>

**Figure 2.** Stability order of  $\text{CH}_3\text{NH}_3\text{PbX}_3$  for  $X = \text{Cl}, \text{Br}, \text{I}$  with respect to different processes.

negative entropy changes cause  $\Delta_r G^\circ$  of reaction 1 to increase with  $T$ , and the decomposition to become more and more disfavored with increasing temperature. It is interesting to note that the largely negative  $\Delta_r S^\circ(1)$  values are related to the high absolute entropies of the  $\text{CH}_3\text{NH}_3\text{PbX}_3$  phases, in turn due to the high entropy changes associated with the phase transitions in the crystal.

Since reaction 1 involves pure solid phases,  $\Delta_r G^\circ$  is practically coincident with the thermodynamic driving force for decomposition,  $\Delta_r G$ , provided that pressure is not too high. The last column of Table 1 indicates the stability of perovskite compounds with respect to precursors of reaction 1. On the basis of the available information, it is concluded that for  $X = \text{Cl}$  and  $\text{Br}$  decomposition is thermodynamically disfavored at 298 K, whereas for  $X = \text{I}$  the results are conflicting: depending on the selected enthalpy change, the negative entropic term can compensate it or not. On the basis of the agreement with tensimetric values, it seems reasonable to recommend provisionally the calorimetric results of Ivanov et al.,<sup>25</sup> which provide the following expressions for the  $\Delta_r G^\circ$  of decomposition reaction 1:

$$\Delta_r G^\circ(\text{CH}_3\text{NH}_3\text{PbCl}_3)(1) = (4.45 + 38.7710^{-3}T) \text{ kJ/mol} \quad (2)$$

$$\Delta_r G^\circ(\text{CH}_3\text{NH}_3\text{PbBr}_3)(1) = (6.78 + 39.9010^{-3}T) \text{ kJ/mol} \quad (3)$$

The so-derived entropy changes  $\Delta_r S^\circ(1)$  at 298 K, also reported in Table 1, are significantly negative (Figure 1) and therefore give a large positive contribution to the decomposition Gibbs energy change, in most cases larger than the enthalpic term, so stabilizing the perovskite phases with respect

to precursors. Furthermore, since  $\left(\frac{\partial \Delta_r G^\circ}{\partial T}\right)_{P=P^\circ} = -\Delta_r S^\circ$ ,

$$\Delta_r G^\circ(\text{CH}_3\text{NH}_3\text{PbI}_3) (1) = (-1.91 + 39.6010^{-3}T) \text{ kJ/mol} \quad (4)$$

189 valid for the room temperature phases (cubic phase for  
190  $\text{CH}_3\text{NH}_3\text{PbCl}_3$  and  $\text{CH}_3\text{NH}_3\text{PbBr}_3$  and tetragonal for  
191  $\text{CH}_3\text{NH}_3\text{PbI}_3$ ) in a reasonably large temperature range (the  
192 temperature dependence of  $\Delta_r H^\circ$  and  $\Delta_r S^\circ$  is not accounted  
193 for in the above equations), including temperatures of practical  
194 interest for photovoltaic devices (typically in the range 30–80  
195 °C). According to these expressions, the perovskite phases are  
196 stable at room temperature, and their stability increases at  
197 higher temperature. In principle, by putting  $\Delta_r G$  equal to zero,  
198 the lowest temperature at which the perovskite phases are  
199 stable can be roughly estimated. These temperatures  
200 correspond to the invariant temperatures (at  $P = P^\circ$ ) where  
201 perovskites would coexist in equilibrium with their precursors.  
202 Simple linear extrapolation of eqs 2–4 gives temperatures  
203 extremely low or even negative, indicating that no decom-  
204 position occurs in practice (obviously, both  $\text{CH}_3\text{NH}_3\text{PbX}_3$  and  
205 the decomposition products would undergo transitions to the  
206 low-temperature phases at the corresponding transition  
207 temperatures). It is then clear from this analysis, that  
208 perovskite phases are “high temperature compounds” in the  
209 pseudobinary  $\text{PbX}_2\text{-CH}_3\text{NH}_3\text{X}$  phase diagram, and reaction 1  
210 should not be regarded as a “thermal” decompositions at all.  
211 However, if the  $\Delta_r H^\circ$  value of ref 26 is used for the iodide  
212 phase, a minimum temperature of stability of 870 K is  
213 estimated by rough extrapolation (even higher than the  
214 melting point of  $\text{PbI}_2$ ), meaning that the material is completely  
215 unsuitable for photovoltaic applications (unless strong kinetic  
216 hindrance comes into play).

218 As mentioned, ascertaining the stability of a material  
219 referring to only one or several processes is not a conclusive  
220 proof of its absolute intrinsic stability. For example, in order to  
221 identify the most favored among a number of possible  
222 decomposition pathways of  $\text{CH}_3\text{NH}_3\text{PbI}_3$ , a convex hull  
223 approach was used, leading to select the decomposition to  
224  $\text{NH}_4\text{I} + \text{PbI}_2 + \text{CH}_2$  as the most stable path.<sup>43</sup> In this  
225 connection, it is interesting to note that the cleavage of the C–  
226 N bond with formation of hydrocarbon fragments  $-\text{CH}_2-$  was  
227 recently observed in *in situ*-deposited  $\text{CH}_3\text{NH}_3\text{PbI}_3$  films by  
228 near ambient pressure XPS.<sup>44</sup>

229 Another process that is sometimes taken as representative of  
230 the intrinsic stability of a material is the opposite of the  
231 formation from elements,  $\text{Pb} + 1.5 \text{X}_2 + 3 \text{H}_2 + 0.5 \text{N}_2 + \text{C} =$   
232  $\text{CH}_3\text{NH}_3\text{PbX}_3$ , with all species in their reference phase (at the  
233 temperature of interest) and in the standard state (see Figure  
234 1).<sup>45</sup> Consistent with eqs 2–4, the following expressions can  
235 be derived for  $\Delta_r G^\circ$  of the  $\text{CH}_3\text{NH}_3\text{PbX}_3$  compounds, valid for  
236 the room temperature phases in a reasonably large temperature  
237 range:

$$\Delta_r G^\circ(\text{CH}_3\text{NH}_3\text{PbCl}_3) = (-662.2 + 579.110^{-3}T) \text{ kJ/mol} \quad (5)$$

$$\Delta_r G^\circ(\text{CH}_3\text{NH}_3\text{PbBr}_3) = (-543.1 + 437.010^{-3}T) \text{ kJ/mol} \quad (6)$$

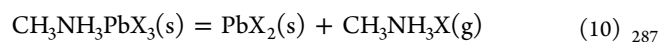
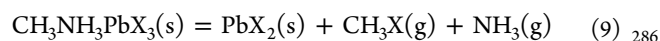
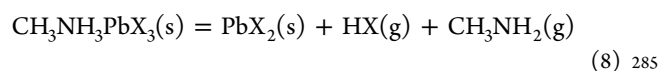
$$\Delta_r G^\circ(\text{CH}_3\text{NH}_3\text{PbI}_3) = (-371.6 + 358.110^{-3}T) \text{ kJ/mol} \quad (7)$$

241 These equations indicate that  $\Delta_r G^\circ$  is strongly negative at  
242 temperatures close to room temperature and show the  
243 expected trend of stability with respect to elements,  $\text{Cl} > \text{Br}$   
244  $> \text{I}$  (Figure 2). Equations 5–7 can be combined with the

corresponding expressions for other substances ( $\text{H}_2\text{O}$ ,  $\text{PbO}$ ,  
245  $\text{PbCO}_3$ ,  $\text{HI}$ ,  $\text{CH}_3\text{NH}_2$ , etc.) to estimate the standard Gibbs  
246 energy change of chemical reactions potentially involved in the  
247 intrinsic or extrinsic (e.g., due to water or oxygen) degradation  
248 of the materials as well in synthesis and annealing processes.  
249 Note that for several important reactions (for example, those  
250 forming perovskite hydrate phases such as  $(\text{CH}_3\text{NH}_3)_4\text{PbI}_6 \cdot$   
251  $2\text{H}_2\text{O}$  under exposure to moisture)  $\Delta_r G^\circ$  cannot be evaluated  
252 owing to the lack of relevant thermodynamic data.

253 In view of the above discussion, the decomposition  
254 processes (1) should not be a worrisome decomposition  
255 path as far as methylammonium lead chloride and bromide  
256 perovskites are concerned, whereas the discrepancy between  
257 calorimetric data makes a conclusive assessment for iodide  
258 difficult. However, other decomposition channels could be at  
259 work under operative conditions. In particular, gas-releasing  
260 decomposition processes are of crucial importance for  
261 investigating the stability of  $\text{CH}_3\text{NH}_3\text{PbX}_3$  and similar  
262 materials. Grazing-incidence wide-angle X-ray diffraction  
263 measurements have shown recently<sup>46</sup> that the dramatic heat-  
264 induced performance decrease of encapsulated perovskite-  
265 based devices is due to surface modifications related to the  
266 intercalation of thermally decomposed methylammonium  
267 fragments into  $\text{PbI}_2$  planes. Since encapsulation is expected  
268 to prevent interaction with external agents, this is a clear  
269 evidence of intrinsically driven degradation related to the loss  
270 of volatile fragments, as already suggested in previous  
271 papers.<sup>22,24</sup> Furthermore, the type of gas that these materials  
272 tend to lose under heating may be of interest for real devices  
273 because gaseous products could interact with the sealing  
274 materials and with the other components of the cell. Finally,  
275 gas-phase releasing degradation is very important under  
276 conditions where the system is allowed to vaporize, such as  
277 postsynthesis annealing<sup>47</sup> and synthesis by vapor deposition  
278 techniques.<sup>48</sup> In spite of this, the direct experimental study of  
279 the released gaseous species has been the subject of relatively  
280 few studies that, unfortunately, presented problematic  
281 results.<sup>27,49,50</sup>

282 In this connection, the following gas-releasing processes are  
283 worth considering:



288 In all three cases, solid lead dihalide is formed, as invariably  
289 observed by means of solid state techniques,<sup>27</sup> and the  
290  $\text{CH}_3\text{NH}_3\text{X}$  portion of the perovskite phase is lost, either as  
291 undissociated methylammonium halide or in the form of  
292 smaller molecules. In principle, gas-phase dissociation can  
293 occur by formation of  $\text{HX}$  or  $\text{CH}_3\text{X}$ , depending on whether the  
294 methyl group or the proton associates with the halide ion.  
295 Theoretical analyses indicate as an energetically favored path  
296 to this kind of degradation the creation of  $\text{HI}$  vacancies and the  
297 subsequent combination of the amine fragment with  $\text{Pb}$  atoms,  
298 which disintegrates the inorganic framework.<sup>51</sup>

299 That the heat-induced degradation of  $\text{CH}_3\text{NH}_3\text{PbI}_3$  perov-  
300 skites proceeds through mass loss has been shown by a number  
301 of thermogravimetric (TGA) measurements and has been also  
302 inferred by solid state techniques, for example by measuring

303 the evolution of I/Pb and N/Pb ratios by photoelectron  
304 spectroscopy.<sup>20</sup>

305 Most investigations of the degradation of CH<sub>3</sub>NH<sub>3</sub>PbX<sub>3</sub> to  
306 volatile species were carried out by classic TGA, where the

Most investigations of the degradation of CH<sub>3</sub>NH<sub>3</sub>PbX<sub>3</sub> to volatile species were carried out by classic TGA, where the mass loss rate is recorded as a function of temperature, usually under an inert dynamic atmosphere

307 mass loss rate is recorded as a function of temperature, usually  
308 under an inert dynamic atmosphere. A number of early TGA  
309 measurements<sup>23,52–54</sup> led to the conclusion that thermal  
310 decomposition of CH<sub>3</sub>NH<sub>3</sub>PbX<sub>3</sub> compounds begins at rather  
311 high temperature, above 200–250 °C, giving support to the  
312 view that the intrinsic thermal stability was not a major  
313 drawback in real applications where temperature does not  
314 exceed 80–90 °C. Various authors also showed that mass loss  
315 starts at lower temperatures for chloride and mixed iodide–  
316 chloride compounds compared to bromide and iodide.<sup>26,54</sup> In  
317 the same years some papers based on XRD and other solid-  
318 state techniques were less optimistic<sup>22,55</sup> pointing out that also  
319 at temperatures as low as 85–100 °C appreciable decom-  
320 position occurred even under an inert atmosphere, especially  
321 under prolonged heating. Actually, the dynamic nature of TGA  
322 experiments, especially if the used scan rate is not very low,  
323 could be insufficient for assessing the long-term stability of a  
324 photovoltaic material, which is required to work for a long time  
325 at temperatures lower than the decomposition temperatures  
326 detectable by TGA curves. Furthermore, the TGA method  
327 does not permit distinguishing among processes 8–10, and the  
328 attribution of the chemical nature of the gaseous phase has  
329 been basically speculative or indirect in the literature, with  
330 reaction 8 generally preferred on the basis of chemical wisdom  
331 (acid–base interaction between the organic cation and the  
332 halide anion). Two-step TGA curves observed by some  
333 authors for CH<sub>3</sub>NH<sub>3</sub>PbI<sub>3</sub> suggested the sequential loss of  
334 HI(g) and CH<sub>3</sub>NH<sub>2</sub>(g),<sup>23</sup> supporting this hypothesis.

335 To the best of our knowledge, the first reports on the direct  
336 detection of the gas phase released by the CH<sub>3</sub>NH<sub>3</sub>PbX<sub>3</sub>  
337 perovskites appeared in 2016,<sup>27,49,54</sup> although FTIR spectroscopy  
338 experiments were previously reported for the vaporization  
339 of dimethylformamide-CH<sub>3</sub>NH<sub>3</sub>PbCl<sub>x</sub>I<sub>3–x</sub> solutions.<sup>56</sup>

340 Extensive vaporization experiments were first reported based  
341 on the classic Knudsen Effusion Mass Loss (KEML) and  
342 Knudsen Effusion Mass Spectrometry (KEMS) techniques.<sup>27</sup>  
343 KEMS measurements were carried out on all three  
344 CH<sub>3</sub>NH<sub>3</sub>PbX<sub>3</sub> compounds in the overall temperature range  
345 76–144 °C, much lower than decomposition temperatures  
346 found in TGA measurements. Mass spectra showed the large  
347 dominance of peaks attributable to HX(g) and CH<sub>3</sub>NH<sub>2</sub>(g),  
348 providing strong evidence of the occurrence of reaction 8  
349 previously proposed in ref 54 based on Temperature-  
350 Programmed Desorption experiments. Weakest peaks corre-  
351 sponding to undissociated CH<sub>3</sub>NH<sub>3</sub>X(g) were also detected (it  
352 should be pointed out that electron impact mass spectrometry  
353 could cause the undissociated CH<sub>3</sub>NH<sub>3</sub>X(g) species to break  
354 into smaller fragment ions.). The thermodynamic analysis of

partial pressure data allowed decomposition enthalpies to be  
355 derived for reaction 8 and, thereafter, formation enthalpies of  
356 CH<sub>3</sub>NH<sub>3</sub>PbX<sub>3</sub> perovskites to also be evaluated. The latter were  
357 subsequently found to agree well with calorimetric results (see  
358 Table 1).<sup>25,50</sup> Shortly after, another study<sup>49</sup> was published  
359 where a very different behavior was observed by TGA-Mass  
360 Spectrometry experiments for CH<sub>3</sub>NH<sub>3</sub>PbI<sub>3</sub> and for its  
361 precursor halide, CH<sub>3</sub>NH<sub>3</sub>I, which were found to release  
362 only NH<sub>3</sub>(g) and CH<sub>3</sub>I(g). Although the largest part of TGA-  
363 MS experiments were carried out at much higher temperatures  
364 (300–420 °C) than Knudsen measurements, authors obtained  
365 some indication that the same process would also take place at  
366 temperatures as low as 80 °C, close to those of interest for  
367 photovoltaic applications. Interestingly, the findings of ref 49  
368 confirmed in part those previously obtained by FTIR.<sup>56</sup> FTIR  
369 spectra of the gas phase recorded at 265 °C indicated the  
370 decomposition of solid CH<sub>3</sub>NH<sub>3</sub>I to NH<sub>3</sub>(g) and CH<sub>3</sub>I(g), in  
371 contrast with CH<sub>3</sub>NH<sub>3</sub>Cl and CH<sub>3</sub>NH<sub>3</sub>PbCl<sub>3</sub>, which was  
372 observed to release HCl(g) and CH<sub>3</sub>NH<sub>2</sub>(g).<sup>373</sup>

In order to shed some light on this scanty and discrepant  
374 experimental information, a thermodynamic analysis is useful.<sup>375</sup>

In principle, reactions 8–10 may occur simultaneously,  
376 giving a three-phase monovariant equilibrium with seven  
377 components, two of them thermodynamically independent.  
378 While the absolute values of the partial pressures depend on  
379 the properties of the two condensed phases, the thermody-  
380 namic competition between the three reactions is basically due  
381 to the different stability of the gaseous species.<sup>382</sup>

Using relations 5–7 for the Gibbs energy of formation of the  
383 perovskite phases and the corresponding well-established  
384 expressions for the products of reactions 8 and 9, the results  
385 reported in Table 2 are derived for the corresponding standard  
386

**Table 2. Standard Gibbs Energy Changes ( $\Delta_r G^\circ$ , in kJ/mol) for the Decomposition Reactions of CH<sub>3</sub>NH<sub>3</sub>PbX<sub>3</sub> and CH<sub>3</sub>NH<sub>3</sub>X with Release of Gaseous Products<sup>a</sup>**

X	CH <sub>3</sub> NH <sub>3</sub> PbX <sub>3</sub> (s) = PbX <sub>2</sub> (s) + HX(g) + CH <sub>3</sub> NH <sub>2</sub> (g) (8)	CH <sub>3</sub> NH <sub>3</sub> PbX <sub>3</sub> (s) = PbX <sub>2</sub> (s) + CH <sub>3</sub> X(g) + NH <sub>3</sub> (g) (9)
Cl	187.9 – 252.3 × 10 <sup>-3</sup> T	174.9 – 249.6 × 10 <sup>-3</sup> T
Br	206.9 – 253.3 × 10 <sup>-3</sup> T	183.3 – 250.3 × 10 <sup>-3</sup> T
I <sup>b</sup>	200.2 – 250.1 × 10 <sup>-3</sup> T	164.7 – 247.2 × 10 <sup>-3</sup> T
X	CH <sub>3</sub> NH <sub>3</sub> X(s) = HX(g) + CH <sub>3</sub> NH <sub>2</sub> (g)	CH <sub>3</sub> NH <sub>3</sub> X(s) = CH <sub>3</sub> X(g) + NH <sub>3</sub> (g)
Cl	183.5 – 291.1 × 10 <sup>-3</sup> T	170.5 – 288.3 × 10 <sup>-3</sup> T
Br	200.1 – 293.3 × 10 <sup>-3</sup> T	176.6 – 290.3 × 10 <sup>-3</sup> T
I	204.7 – 289.7 × 10 <sup>-3</sup> T	169.2 – 286.8 × 10 <sup>-3</sup> T

<sup>a</sup>These expressions can be applied in a reasonably large temperature range near to 298 K. <sup>b</sup>Cubic phase of CH<sub>3</sub>NH<sub>3</sub>PbI<sub>3</sub>.

Gibbs energy changes. Data in Table 2 indicate that, at  
387 variance with the trend of formation enthalpies, bromide is the  
388 most stable with respect to vaporization decomposition  
389 (Figure 2) for both processes 8 and 9. However, the stability  
390 trend is Br > I > Cl and Br > Cl > I, respectively, for the two  
391 processes. Note that only in the case of reaction 8 is the  
392 stability order in agreement with TGA experiments (see  
393 above). For the sake of comparison, in the same table, the  
394  $\Delta_r G^\circ$ 's are also reported for the corresponding decomposition  
395 reactions of methylammonium halides, CH<sub>3</sub>NH<sub>3</sub>X. It is  
396 interesting to note that  $\Delta_r G^\circ$  values for the latter are lower  
397 (i.e., the decomposition pressures are higher for a given  
398 temperature) than those of the corresponding perovskites. A  
399

400 large part of this effect is due to the higher entropy changes for  
401 the decomposition of  $\text{CH}_3\text{NH}_3\text{X}$  compounds.

402 A similar analysis for process 10 is made difficult by the lack  
403 of thermodynamic data for the species  $\text{CH}_3\text{NH}_3\text{X}(\text{g})$ , which is  
404 not surprising if we consider that, even for the simpler  
405 ammonium halide species,  $\text{NH}_4\text{X}(\text{g})$ , experimental data are  
406 more uncertain than one might believe. For example, the  
407 dissociation degree of  $\text{NH}_4\text{Cl}(\text{g})$  to  $\text{NH}_3(\text{g})$  and  $\text{HCl}(\text{g})$  has  
408 been the subject of a longstanding debate, with experimental  
409 results ranging from complete to very limited dissociation and  
410 theoretical studies claiming for a fair stability of the  
411 undissociated hydrogen-bond linked species.<sup>57</sup> Although the  
412  $\text{CH}_3\text{NH}_2 + \text{HCl}$  potential energy surface has been the subject  
413 of a number of theoretical studies aimed at clarifying the  
414 mechanism of the methyl exchange in solution phase (the so-  
415 called Menshutkin  $\text{S}_{\text{N}}2$  reaction,  $\text{CH}_3\text{Cl} + \text{NH}_3 =$   
416  $\text{CH}_3\text{NH}_3^+\text{Cl}^-$ ), apparently a stable structure for the  
417  $\text{CH}_3\text{NH}_3\text{Cl}$  complex in the gas phase was reported only  
418 recently by Patterson<sup>58</sup> based on DFT calculations. In order to  
419 evaluate the relative importance of reaction 10 for the iodide  
420 perovskite under thermodynamic conditions, similar calcu-  
421 lations were done for the  $\text{CH}_3\text{NH}_3\text{I}(\text{g})$  species,<sup>59</sup> that allowed  
422 us to derive an approximate estimate of  $\Delta_r G^\circ(10)$  as

$$\Delta_r G^\circ(10) = (143.8 - 111.310 - 3T) \text{ kJ/mol} \quad (\text{X} = \text{I}) \quad (11)$$

423 (cubic phase of  $\text{CH}_3\text{NH}_3\text{PbI}_3$ ). From the equations in Table 2  
424 and eq 11, the partial pressures of all the gaseous species in  
425 equilibrium with  $\text{CH}_3\text{NH}_3\text{PbI}_3$  and  $\text{PbI}_2$  were estimated. The  
426 so-derived *total* pressures produced from reactions 8–10 are  
427 reported in Figure 3 along with the total pressures measured by  
428 the classic Knudsen effusion method<sup>27,60</sup> (the only exper-  
429 imental value available to date). This plot shows clearly that,  
430 under the hypothesis of thermodynamic equilibrium, the  
431 decomposition channel of  $\text{CH}_3\text{NH}_3\text{PbI}_3$  leading to  $\text{NH}_3 +$   
432  $\text{CH}_3\text{I}$  (process 9) should be by far the most important,

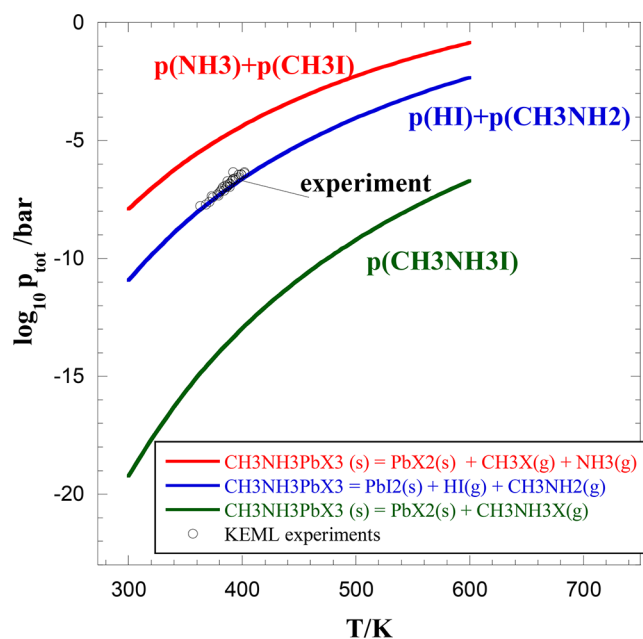


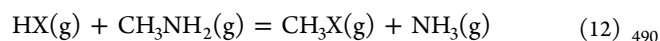
Figure 3. Total pressures produced by decomposition processes 8–10 evaluated from calorimetric data, compared to the results of KEML experiments.<sup>27,60</sup>

especially at moderate temperatures, followed by that one  
releasing  $\text{CH}_3\text{NH}_2 + \text{HI}$  and eventually by the evaporation to  
the undissociated species, which is negligible at any temper-  
ature of interest. However, the decomposition pressure due to  
the loss of  $\text{NH}_3 + \text{CH}_3\text{I}$  should be 2–3 orders of magnitude  
higher than that experimentally observed under effusion  
conditions, which instead agrees well with the occurrence of  
process 8. It should be pointed out that our thermodynamic  
prediction is entirely based on calorimetric results (eqs 5–7).  
Being such data are completely independent from tensimetric  
measurements, the agreement with the latter is very  
satisfactory. It should also be pointed out that our calculation  
for process 10 is based on computationally estimated  
thermodynamic data.

Overall, from this analysis the conclusion can be drawn that  
(i) process 9 has a much larger thermodynamic driving force,  
but (ii) under effusion conditions, which, in principle, should  
allow an approach toward thermodynamic equilibrium, the  
occurrence of this process is kinetically hindered, and the  
measured pressures suggests that process 8 takes place instead.  
The kinetic limitation of reactions 9 seems quite plausible  
because the breaking of a strong C–N bond (330 kJ/mol at  
298 K) is required, instead of the hydrogen-bond breaking  
involved in process 8. This view is supported by DFT  
calculations,<sup>49</sup> which predict a remarkable activation barrier for  
reaction 9, and by the comparison with the thermal  
decomposition behavior of simple alkylammonium halides  
(see below). It should be noted that the very good agreement  
between calculated and experimental data indicates that, as far  
as process 8 is concerned, thermodynamic equilibrium is fully  
attained under Knudsen conditions, giving confidence in the  
thermodynamic properties derived from tensimetric measure-  
ments, provided that data are analyzed on the basis of the  
proper reaction.

In view of the above analysis, the aforementioned  
experimental results on the decomposition of  $\text{CH}_3\text{NH}_3\text{PbX}_3$   
(especially in regard to  $\text{CH}_3\text{NH}_3\text{PbI}_3$ ) are somehow puzzling.  
Apparently, measurements under Knudsen conditions, which  
are supposed to favor the attainment of thermodynamic  
equilibrium, gave evidence for the occurrence of the  
thermodynamically disfavored process 8, whereas “open-pan”  
TGA-MS and IR experiments provided evidence for the  
occurrence of the thermodynamic pathway. Since the latter  
experiments were mostly performed in a much higher  
temperature range where kinetic hindrance might be over-  
come, the question arises whether different temperatures alone  
can account for the experimental findings or other effects are to  
be invoked, such as vacuum versus dynamic inert atmosphere,  
heating scan versus thermal equilibration, presence of a heated  
transfer line, etc.

More recent KEMS experiments<sup>50</sup> where the competition  
between processes 8 and 9 was studied by measuring the  
 $p(\text{HI})/p(\text{CH}_3\text{I})$  ratio under different conditions, provided  
some additional information. The competition between the  
two processes is basically driven by the following homoge-  
neous pressure-independent gaseous equilibrium:<sup>50</sup>



Since the gaseous species come in 1:1 molar ratio from the  
 $\text{CH}_3\text{NH}_3\text{PbX}_3$  solid, at equilibrium  $p(\text{HX}) = p(\text{CH}_3\text{NH}_2) \equiv$   
 $p(8)$  and  $p(\text{CH}_3\text{X}) = p(\text{NH}_3) \equiv p(9)$ , with

$$\frac{p(8)}{p(9)} = \exp\left(\frac{\Delta_r G^\circ(12)}{2RT}\right) \quad (13)$$

In view of the small entropy change of reaction 12, the partial pressure ratio 13 is ruled by the enthalpic factor. Since ammonia is much more thermally stable than methylamine ( $\Delta_f H_{298}^\circ = -45.94$  and  $-22.5$  kJ/mol, respectively), at the temperatures of interest equilibrium 12 is shifted toward the right, regardless of the nature of X. Furthermore, since HI is thermally unstable ( $\Delta_f H_{298}^\circ = +26.5$  kJ/mol) compared to  $\text{CH}_3\text{I}$  ( $\Delta_f H_{298}^\circ = 14.4$  kJ/mol), the decomposition channel 8 is especially disfavored for iodide. The reverse holds for chloride ( $\Delta_f H_{298}^\circ = -92.3$  and  $-81.9$  kJ/mol for HCl and  $\text{CH}_3\text{Cl}$ , respectively), whereas the thermal stabilities of  $\text{CH}_3\text{Br}$  and HBr are practically equal ( $\Delta_f H_{298}^\circ = -36.3$  and  $-36.4$  kJ/mol). Being exothermic, reaction 12 tends to shift to left at higher temperatures, although right-hand products remain strongly favored at any temperature of interest. In Figure 4, the  $p(\text{HI})/$

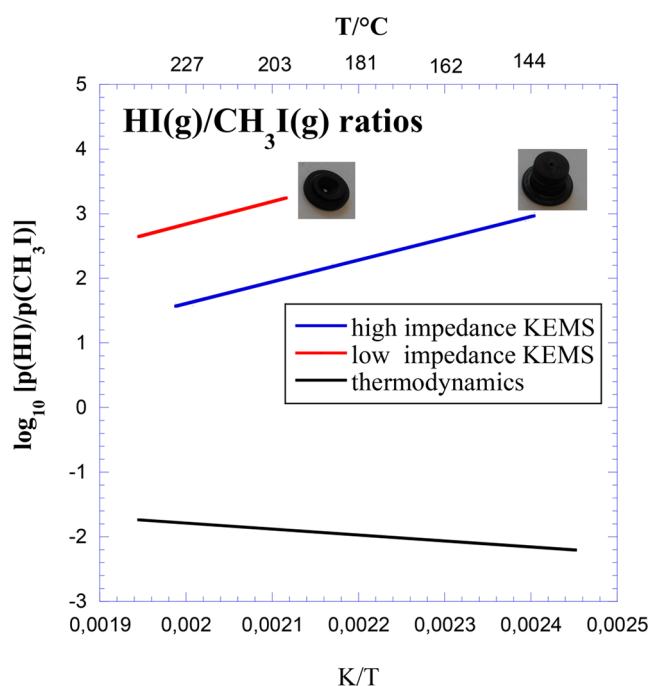


**Figure 4.**  $\text{HI}(\text{g})/\text{CH}_3\text{I}(\text{g})$  partial pressures ratios illustrating the competition between the decomposition processes 8 and 9. Red and blue lines refer to KEMS measurements performed, respectively, with low flow impedance (ordinary effusion cap) and high flow impedance (chimney-like cap).<sup>50</sup>

$p(\text{CH}_3\text{I})$  pressure ratio calculated by eq 13 is reported, along with the corresponding ratios measured by KEMS in a higher temperature range compared to ref 27, using two different effusion caps.<sup>50</sup> The red line refers to experiment carried out with an ordinary effusion hole (1 mm diameter, negligible thickness), the blue one was derived using a sort of “chimney” orifice, with 0.5 mm in diameter and a 6.5 mm long channel making the effusion rate lower (see the cap pictures in Figure 4). The higher impedance to effusion flow is expected to favor approaching the heterogeneous equilibrium. Indeed, Figure 4 clearly shows that (i) higher temperatures do favor the formation of  $\text{CH}_3\text{I}(\text{g})$  versus  $\text{HI}(\text{g})$ , contrarily to thermodynamic predictions (black line with negative slope in Figure 4), and (ii) high impedance effusion conditions have the same

effect, decreasing the  $\text{HI}/\text{CH}_3\text{I}$  ratio by more than 1 order of magnitude. A schematic picture of these findings is reported in Figure 5. Nevertheless, under all the explored conditions,

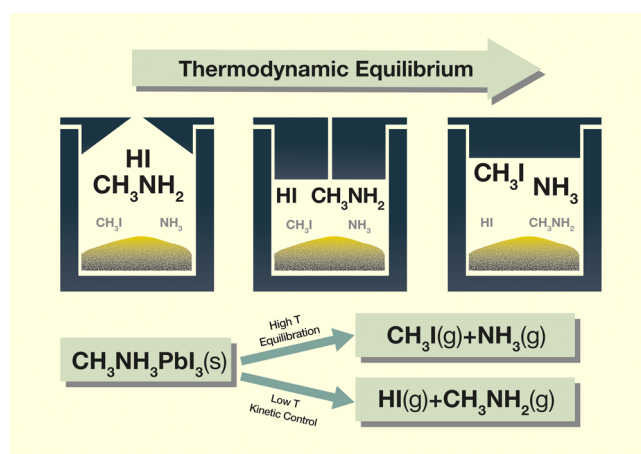
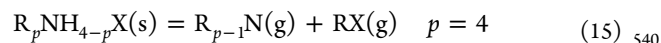
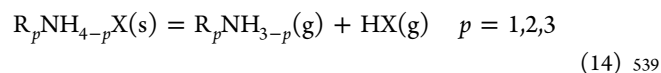


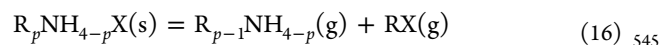
**Figure 5.** Graphic representation of the experimental conditions leading to kinetically controlled (process 8) or thermodynamically controlled (process 9) decomposition pathways. Higher temperatures and/or closer-to-equilibrium conditions favor the thermodynamic control.<sup>50</sup>

process 8 remains the dominant decomposition pathway. Therefore, according to KEMS results, even at temperature as high as 250 °C, process 9 cannot come out by the extent predicted by equilibrium thermodynamics.

In an attempt to rationalize the observed decomposition behavior of  $\text{CH}_3\text{NH}_3\text{PbX}_3$  perovskites, a possible benchmark is given by the thermal decomposition of simple mono- di-, tri-, and tetraalkylammonium halides, which have been the subject of quite a high number of studies.<sup>61–63</sup> On the basis of TGA experiments, Błażejowski and co-workers concluded that compounds of general formula  $\text{R}_p\text{NH}_{4-p}\text{X}$  decompose under heating according to the following processes:<sup>62</sup>



In other words, mono-, di- and trialkyl ammonium halides decompose, releasing the corresponding amine and hydrogen halide rather than by the alternative process releasing the alkyl halide and the less substituted amine:



whereas tetraalkylammonium halides, which do not contain hydrogen atoms, decompose by loss of alkyl halide and trialkylamine. The occurrence of the latter process was also confirmed by direct FTIR spectroscopy experiments.<sup>63</sup>

As far as thermodynamic equilibrium is concerned, the above-reported discussion on the competition between processes 8 and 9 could be extended to processes 14 and 16. Actually, the pressure ratio (process 12) in equilibrium with the  $\text{CH}_3\text{NH}_3\text{PbX}_3 + \text{PbX}_2$  mixture is the same as that in equilibrium with the methylammonium halide solids  $\text{CH}_3\text{NH}_3\text{X}$ , and it is ruled by the relative stability of  $\text{NH}_3(\text{g})$  versus  $\text{CH}_3\text{NH}_2(\text{g})$  and  $\text{HX}(\text{g})$  versus  $\text{CH}_3\text{X}(\text{g})$ , which would strongly favor process 16 (see above). Other cases can be more complex, since the relative stability of  $\text{HX}(\text{g})$  and  $\text{RX}(\text{g})$

560 depends markedly on  $X$  and that of  $R_p\text{NH}_{3-p}(\text{g})$  versus  
561  $R_{p-1}\text{NH}_{4-p}(\text{g})$  for  $p = 2,3$  is not obvious.

562 The kinetic hindrance of the C–N bond-breaking process  
563 involved in decomposition reactions 15 and 16 is supported by  
564 the fact that quaternary amines, where process 14 cannot take  
565 place, are observed to decompose at much higher temperatures  
566 than less substituted compounds.<sup>63</sup> Furthermore, the enthalpy  
567 changes of the thermal decomposition of tetraalkylammonium  
568 halides as measured by TGA have been found to be much  
569 higher than those measured by DSC (for instance, 319.7 kJ/  
570 mol versus 186.7 kJ/mol for  $(\text{CH}_3)_4\text{NI}$ <sup>63</sup>), which correspond  
571 to the actual energy required to convert the solid into gaseous  
572 products (i.e., the thermodynamic decomposition enthalpy). In  
573 TGA measurements, where the enthalpy change is obtained by  
574 the temperature dependence of the mass loss rate, the  
575 activation barrier is instead measured. DFT calculations fully  
576 support this view. For example, an activation energy of 239 kJ/  
577 mol was calculated recently<sup>64</sup> for the thermodynamically  
578 favored decomposition of dioctylammonium chloride to  
579 dioctylamine +1-chlorooctane, whereas no activation barrier  
580 is found for the alternative process leading to trioctylammo-  
581 nium chloride and HCl. While the outlined frame of the  
582 thermal behavior of alkylammonium halide seems fairly well-  
583 established, nonetheless the direct experimental evidence of  
584 process 14 for mono-, di-, and trisubstituted compounds seems  
585 scarce, and indeed recent perovskite-related experiments seem  
586 to call it into question.<sup>49,56</sup>

587 In conclusion, the intrinsic stability of  $\text{CH}_3\text{NH}_3\text{PbX}_3$   
588 perovskites can be analyzed in the light of a classical  
589 thermodynamic analysis relying on the limited experimental  
590 information available to date. Decomposition reactions to solid  
591 precursors  $\text{PbX}_2(\text{s})$  and  $\text{CH}_3\text{NH}_3\text{X}(\text{s})$  are shown to be  
592 thermodynamically disfavored for  $X = \text{Cl}, \text{Br}$ , in great part  
593 because of the large negative decomposition entropies. For  $X =$   
594  $\text{I}$ , the serious discrepancy between the calorimetric determi-  
595 nations does not allow one to draw definitive conclusions on  
596 the thermodynamic driving force of this decomposition  
597 pathway, although the entropic contribution certainly also  
598 plays a large stabilizing role in this case. Decomposition  
599 reactions are most likely to occur by the release of gaseous  
600 products, a process that, according to recent experimental  
601 findings, may play an important role even in encapsulated  
602 devices. However, the identification of the molecular species  
603 lost by the perovskite structure is still uncertain, and the  
604 limited experimental information is not conclusive. Decom-  
605 position to  $\text{NH}_3(\text{g})$  and  $\text{CH}_3\text{X}(\text{g})$  is largely favored from a  
606 thermodynamic point of view, but it seems to suffer from a  
607 severe kinetic limitation related to the breaking of the strong  
608 C–N bond in the organic cation, as previously observed in the  
609 thermal decomposition of alkylammonium halides. Indeed,  
610 TGA-MS measurements support the occurrence of this  
611 decomposition channel at high temperature. However, effusion  
612 experiments indicate, in spite of thermodynamic driving forces,  
613 the release of  $\text{HX}(\text{g})$  and  $\text{CH}_3\text{NH}_2(\text{g})$ , rather than  $\text{NH}_3(\text{g})$   
614 and  $\text{CH}_3\text{X}(\text{g})$ , at temperatures much lower than the  
615 decomposition temperatures detected by TGA experiments.  
616 The thermodynamic pathway becomes more important at  
617 higher temperature and under closer-to-equilibrium effusion  
618 conditions. The release of undissociated  $\text{CH}_3\text{NH}_3\text{X}(\text{g})$   
619 molecules seems thermodynamically disfavored, although  
620 accurate thermodynamic data for these species are lacking.  
621 While thermodynamics prove to be very useful in rationalizing  
622 the degradation behavior of perovskite materials and

corresponding precursors, careful attention has to be paid to 623  
kinetic effects. However, the scarcity and the uncertainty of the 624  
experimental data currently available is a serious limit to 625  
thermodynamic predictions, which would greatly benefit from 626  
increased research efforts aimed at determining accurate 627  
thermodynamic information by independent techniques 628  
under various conditions. It is desirable that, in the next 629  
years, chemical thermodynamics research will give a greater 630  
contribution to assess the stability and the suitability of 631  
perovskite materials for photovoltaics and, more generally, to 632  
help the development of advanced materials for energy 633  
applications.<sup>65</sup> 634

## 635 AUTHOR INFORMATION

### 636 Corresponding Author

\*E-mail: [andrea.ciccioli@uniroma1.it](mailto:andrea.ciccioli@uniroma1.it). 637

### 638 ORCID

Andrea Ciccioli: 0000-0003-1421-8062 639

Alessandro Latini: 0000-0002-3205-4826 640

### 641 Notes

The authors declare no competing financial interest. 642

### 643 Biographies

644 **Andrea Ciccioli** (born 1969) is a Senior Scientist at the Department  
645 of Chemistry of the University of Rome “La Sapienza”. His current  
646 research interests include the determination of thermodynamic  
647 properties of condensed phases by tensimetric measurements, the  
648 investigation of the evaporation/decomposition behavior of ionic  
649 liquids and hybrid materials, the experimental and computational  
650 study of bond energies of gaseous molecules.

651 **Alessandro Latini** was born in Rome, Italy, in 1974. He obtained a  
652 Master degree in Chemistry and a Ph.D. in Chemical Sciences (2006)  
653 from the University of Rome “La Sapienza”, where he presently works  
654 as a Senior Scientist. His research is focused on the synthesis,  
655 characterization, and thermodynamic analysis of inorganic and hybrid  
656 materials, with special focus on advanced materials for energy  
657 conversion. He has coauthored 62 publications in international peer-  
658 reviewed journals.

## 659 ACKNOWLEDGMENTS

660 Authors wish to thank warmly Prof. Eric V. Patterson (Stony  
661 Brook University, New York, USA) for sharing unpublished  
662 computational results on the  $\text{CH}_3\text{NH}_3\text{I}(\text{g})$  dissociation  
663 reaction, and Prof. Rohan Mishra (Washington University in  
664 St. Louis, St. Louis, Missouri, USA) for providing numerical  
665 values of the theoretical decomposition enthalpies of  
666  $\text{CH}_3\text{NH}_3\text{PbX}_3$ . The work done by Mr. Niccolò Iacovelli in  
667 preparing Figures 1, 2, 5, and the TOC/abstract graphic is  
668 gratefully acknowledged.

## 669 REFERENCES

- 670 (1) Asghar, M. I.; Zhang, J.; Wang, H.; Lund, P. D. Device Stability  
671 of perovskite Solar Cells: A review. *Renewable Sustainable Energy Rev.*  
672 **2017**, *77*, 131–146.
- 673 (2) Berhe, T. A.; Su, W.-N.; Chen, C.-H.; Pan, C.-J.; Cheng, J.-H.;  
674 Chen, H.-M.; Tsai, M.-C.; Chen, L.-Y.; Dubale, A. A.; Hwang, B.-J.  
675 Organometal Halide Perovskite Solar Cells: Degradation and Stability.  
676 *Energy Environ. Sci.* **2016**, *9*, 323–356.
- 677 (3) Manser, J. S.; Saidaminov, M. I.; Christians, J. A.; Bakr, O. M.;  
678 Kamat, P. V. Making and Breaking of Lead Halide Perovskites. *Acc.*  
679 *Chem. Res.* **2016**, *49*, 330–338.



- (4) Wang, D.; Wright, M.; Elumalai, N. K.; Uddin, A. Stability of perovskite Solar Cells. *Solar Energy Mater. Sol. Energy Mater. Sol. Cells* **2016**, *147*, 255–275.
- (5) Leijtens, T.; Eperon, G. E.; Noel, N. K.; Habisreutinger, S. N.; Petrozza, A.; Snaith, H. J. Stability of Metal Halide Perovskite Solar Cells. *Adv. Energy Mater.* **2015**, *5*, 1500963.
- (6) Niu, G.; Guo, X.; Wang, L. Review of Recent Progress in Chemical Stability of Perovskite Solar Cells. *J. Mater. Chem. A* **2015**, *3*, 8970–8980.
- (7) Ono, L. K.; Juarez-Perez, E. J.; Qi, Y. Progress on Perovskite Materials and Solar Cells with Mixed Cations and Halide Anions. *ACS Appl. Mater. Interfaces* **2017**, *9*, 30197–30246.
- (8) Chen, J.; Cai, X.; Yang, D.; Song, D.; Wang, J.; Jiang, J.; Ma, A.; Lv, S.; Hu, M. Z.; Ni, C. Recent Progress in Stabilizing Hybrid Perovskites for Solar Cell Applications. *J. Power Sources* **2017**, *355*, 98–133.
- (9) Slavney, A. H.; Smaha, R. W.; Smith, I. C.; Jaffe, A.; Umeyama, D.; Karunadasa, H. I. Chemical Approach to Addressing the Instability and Toxicity of Lead-Halide Perovskite Absorbers. *Inorg. Chem.* **2017**, *56*, 46–55.
- (10) Ito, S.; Tanaka, S.; Manabe, K.; Nishino, H. Effects of Surface Blocking Layer of  $\text{Sb}_2\text{S}_3$  on Nanocrystalline  $\text{TiO}_2$  for  $\text{CH}_3\text{NH}_3\text{PbI}_3$  Perovskite Solar Cells. *J. Phys. Chem. C* **2014**, *118*, 16995–17000.
- (11) Matteocci, F.; Cinà, L.; Lamanna, E.; Cacovich, S.; Divitini, G.; Midgley, P. A.; Ducati, C.; Di Carlo, A. Encapsulation for Long-Term Stability Enhancement of Perovskite Solar Cells. *Nano Energy* **2016**, *30*, 162–172.
- (12) Huang, J.; Tan, S.; Lund, P. D.; Zhou, H. Impact of  $\text{H}_2\text{O}$  on Organic-Inorganic Hybrid Perovskite Solar Cells. *Energy Environ. Sci.* **2017**, *10*, 2284–2311.
- (13) Matsumoto, F.; Vorpahl, S. M.; Banks, J. Q.; Sengupta, E.; Ginger, D. S. Photodecomposition and Morphology Evolution of Organometal Halide Perovskite Solar Cells. *J. Phys. Chem. C* **2015**, *119*, 20810–20816.
- (14) Poorkazem, K.; Kelly, T. L. Compositional Engineering to Improve the Stability of Lead Halide Perovskites: A comparative Study of Cationic and Anionic Dopants. *ACS Appl. Energy Mater.* **2018**, *1*, 181–190.
- (15) Ono, L. K.; Qi, Y. Surface and Interface Aspects of Organometal Halide Perovskite Materials and Solar Cells. *J. Phys. Chem. Lett.* **2016**, *7*, 4764–4794.
- (16) Guerrero, A.; You, J.; Aranda, C.; Kang, Y. O.; Garcia-Belmonte, G.; Zhou, H.; Bisquert, J.; Yang, Y. Interfacial Degradation of Planar Lead Halide Perovskite Solar Cells. *ACS Nano* **2016**, *10*, 218–224.
- (17) Huang, W.; Manser, J. S.; Kamat, P. V.; Ptasinska, S. Evolution of Chemical Composition, Morphology, and Photovoltaic Efficiency of  $\text{CH}_3\text{NH}_3\text{PbI}_3$  Perovskite under Ambient Conditions. *Chem. Mater.* **2016**, *28*, 303–311.
- (18) Koocher, N. Z.; Saldana-Greco, D.; Wang, F.; Liu, S.; Rappe, A. M. Polarization Dependence of Water Adsorption to  $\text{CH}_3\text{NH}_3\text{PbI}_3$  (001). *J. Phys. Chem. Lett.* **2015**, *6*, 4371–438.
- (19) Yuan, H.; Debroye, E.; Janssen, K.; Naiki, H.; Steuwe, C.; Lu, G.; Moris, M.; Orgiu, E.; Uji-I, H.; De Schryver, F.; Samori, P.; et al. Degradation of Methylammonium Lead Iodide Perovskite Structures through Light and Electron Beam Driven Ion Migration. *J. Phys. Chem. Lett.* **2016**, *7*, 561–566.
- (20) Philippe, B.; Park, B.-W.; Lindblad, R.; Oscarsson, J.; Ahmadi, S.; Johansson, E. M.; Rensmo, H. Chemical and Electronic Structure Characterization of Lead Halide Perovskite and Stability Behavior under Different Exposures – A Photoelectron Spectroscopy Investigation. *Chem. Mater.* **2015**, *27*, 1720–1731.
- (21) Akbulatov, A. F.; Luchkin, S. Yu.; Frolova, L. A.; Dremova, N. N.; Gerasimov, K. L.; Zhidkov, I. S.; Anokhin, A. V.; Kurmaev, E. Z.; Stevenson, K. J.; Troshin, P. A. Probing the Intrinsic Thermal and Photochemical Stability of Hybrid and Inorganic Lead Halide Perovskites. *J. Phys. Chem. Lett.* **2017**, *8*, 1211–1218.
- (22) Conings, B.; Drijkoningen, J.; Gauquelin, N.; Babayigit, A.; D'Haen, J.; D'Olieslaeger, L.; Ethirajan, A.; Verbeeck, J.; Manca, J.; Mosconi, E.; De Angelis, F.; Boyen, H.-G. Intrinsic Thermal Instability of Methylammonium Lead Trihalide Perovskite. *Adv. Energy Mater.* **2015**, *5*, 1500477.
- (23) Dualeh, A.; Gao, P.; Seok, S. I.; Nazeeruddin, M. K.; Grätzel, M. Thermal Behavior of Methylammonium Lead-Trihalide Perovskite Photovoltaic Light Harvester. *Chem. Mater.* **2014**, *26*, 6160–6164.
- (24) Alberti, A.; Deretzis, I.; Pellegrino, G.; Bongiorno, C.; Smecca, E.; Mannino, G.; Giannazzo, F.; Condorelli, G. G.; Sakai, N.; Miyasaka, T.; et al. Similar Structural Dynamics for the Degradation of  $\text{CH}_3\text{NH}_3\text{PbI}_3$  in Air and in Vacuum. *ChemPhysChem* **2015**, *16*, 3064–3071.
- (25) Ivanov, I. L.; Steparuk, A. S.; Bolyachkina, M. S.; Tsvetkov, D. S.; Safronov, A. P.; Zuev, A. Yu. Thermodynamics of formation of hybrid perovskite-type methylammonium lead halides. *J. Chem. Thermodyn.* **2018**, *116*, 253–258.
- (26) Nagabhushana, G. P.; Shivarajiah, R.; Navrotsky, A. Direct Calorimetric Verification of Thermodynamic Instability of Lead Halide Hybrid Perovskites. *Proc. Natl. Acad. Sci. U. S. A.* **2016**, *113*, 7717–7721.
- (27) Brunetti, B.; Cavallo, C.; Ciccio, A.; Gigli, G.; Latini, A. On the Thermal and Thermodynamic (In)stability of Methylammonium Lead Halide Perovskites. *Sci. Rep.* **2016**, *6*, 31896; Corrigendum: On the Thermal and Thermodynamic (In)Stability of Methylammonium Lead Halide Perovskites. *Sci. Rep.* **2017**, *7*, 46867.
- (28) Thind, A. S.; Huang, X.; Sun, J.; Mishra, R. First-Principle Prediction of a Stable Hexagonal Phase of  $\text{CH}_3\text{NH}_3\text{PbI}_3$ . *Chem. Mater.* **2017**, *29*, 6003–6011.
- (29) Faghianisari, M.; Izadifard, M.; Ghazi, M. E. DFT Study of Mechanical Properties and Stability of Cubic Methylammonium Lead Halide Perovskites ( $\text{CH}_3\text{NH}_3\text{PbX}_3$ , X = I, Br, Cl). *J. Phys. Chem. C* **2017**, *121*, 27059–27070.
- (30) Yang, D.; Lv, J.; Zhao, X.; Xu, Q.; Fu, Y.; Zhan, F.; Zunger, A.; Zhang, L. Functionality-Directed Screening of Pb-Free Hybrid Organic-Inorganic Perovskites with Desired Intrinsic Photovoltaic Functionalities. *Chem. Mater.* **2017**, *29*, 524–538.
- (31) Buin, A.; Comin, R.; Xu, J.; Ip, A. H.; Sargent, E. H. Halide-Dependent Electronic Structure of Organolead Perovskite Materials. *Chem. Mater.* **2015**, *27*, 4405–4412.
- (32) Zhang, Y.-Y.; Chen, S.; Xu, P.; Xiang, H.; Gong, X.-G.; Walsh, A.; Wei, S.-H. Intrinsic Instability of the Hybrid Halide Perovskite Semiconductor  $\text{CH}_3\text{NH}_3\text{PbI}_3$ . *arXiv.org, e-Print Arch., Condens. Matter* **2015**, No. arXiv:1506.01301.
- (33) Buin, A.; Pietsch, P.; Xu, J.; Voznyy, O.; Ip, A. H.; Comin, R.; Sargent, E. H. Materials Processing Routes to Trap-Free Halide Perovskites. *Nano Lett.* **2014**, *14*, 6281–6286.
- (34) Tenuta, E.; Zheng, C.; Rubel, O. Thermodynamic Origin of Instability in Hybrid Halide Perovskites. *Sci. Rep.* **2016**, *6*, 37654.
- (35) Ganose, A. M.; Savory, C. N.; Scanlon, D. O.  $(\text{CH}_3\text{NH}_3)_2\text{Pb}(\text{SCN})_2$ : A More Stable Structural Motif for Hybrid Halide Photovoltaics? *J. Phys. Chem. Lett.* **2015**, *6*, 4594–4598.
- (36) Zheng, C.; Rubel, O. Ionization Energy as a Stability Criterion for Halide Perovskites. *J. Phys. Chem. C* **2017**, *121*, 11977–11984.
- (37) Yang, B.; Dyck, O.; Ming, W.; Du, M.-H.; Das, S.; Rouleau, C. M.; Duscher, G.; Geohegan, D. B.; Xiao, K. Observation of Nanoscale Morphological and Structural Degradation in Perovskite Solar Cells by in Situ TEM. *ACS Appl. Mater. Interfaces* **2016**, *8*, 32333–32340.
- (38) Agiorgousis, M. L.; Sun, Y.-Y.; Zeng, A.; Zhang, S. Strong Covalency-Induced Recombination Centers in Perovskite Solar Cell Material  $\text{CH}_3\text{NH}_3\text{PbI}_3$ . *J. Am. Chem. Soc.* **2014**, *136*, 14570–14575.
- (39) Haruyama, J.; Sodeyama, K.; Han, L.; Tateyama, Y. Termination Dependence of Tetragonal  $\text{CH}_3\text{NH}_3\text{PbI}_3$  Surfaces for Perovskite Solar Cells. *J. Phys. Chem. Lett.* **2014**, *5*, 2903–2909.
- (40) Yin, W.-J.; Shi, T.; Yan, Y. Unusual Defect Physics in  $\text{CH}_3\text{NH}_3\text{PbI}_3$  Perovskite Solar Cell Absorbers. *Appl. Phys. Lett.* **2014**, *104*, 063903.
- (41) Onoda-Yamamuro, N.; Matsuo, T.; Suga, H. Calorimetric and IR Spectroscopic Studies of Phase Transitions in Methylammonium

- 817 Trihalogenoplumbates (II). *J. Phys. Chem. Solids* **1990**, *51*, 1383–  
818 1395.
- 819 (42) Glasser, L.; Jenkins, D. D. B. Standard Absolute Entropies,  
820  $S^\circ_{298}$ , from Volume or Density. Part II. Organic Liquids and Solids.  
821 *Thermochim. Acta* **2004**, *414*, 125–130.
- 822 (43) El-Mellouhi, F.; Bentría, E. T.; Rashkeev, S. N.; Kais, S.;  
823 Alharbi, F. H. Enhancing Intrinsic Stability of Hybrid Perovskite Sola  
824 Cell by Strong, yet Balanced, Electronic Coupling. *Sci. Rep.* **2016**, *6*,  
825 30305.
- 826 (44) Chun-Ren Ke, J.; Walton, A. S.; Lewis, D. J.; Tedstone, A.;  
827 O'Brien, P.; Thomas, A. G.; Flavell, W. R. In situ Investigation of  
828 Degradation at Organometal Halide Perovskite Surfaces by X-Ray  
829 Photoelectron Spectroscopy at Realistic Water Vapour Pressure. *Chem.*  
830 *Commun.* **2017**, *53*, 5231.
- 831 (45) Hong, F.; Saparov, B.; Meng, W.; Xiao, Z.; Mitzi, D. B.; Yan, Y.  
832 Viability of Lead-Free Perovskites with Mixed Chalcogen and  
833 Halogen Anions for Photovoltaic Applications. *J. Phys. Chem. C*  
834 **2016**, *120*, 6435–6441.
- 835 (46) Kim, N.-K.; Min, Y. H.; Noh, S.; Cho, E.; Jeong, G.; Joo, M.;  
836 Ahn, S.-W.; Lee, J. S.; Kim, S.; Ihm, K.; Ahn, H.; et al. Investigation of  
837 Thermally Induced Degradation in  $\text{CH}_3\text{NH}_3\text{PbI}_3$  Perovskite Solar  
838 Cells Using In-situ Synchrotron Radiation Analysis. *Sci. Rep.* **2017**, *7*,  
839 4645.
- 840 (47) Song, Z.; Watthage, S. C.; Phillips, A. B.; Tompkins, B. L.;  
841 Ellingson, R. J.; Heben, M. J. Impact of Processing Temperature and  
842 Composition on the Formation of Methylammonium Lead Iodide  
843 Perovskites. *Chem. Mater.* **2015**, *27*, 4612–4619.
- 844 (48) Leyden, M. R.; Meng, L.; Jiang, Y.; Ono, L. K.; Qiu, L.; Juarez-  
845 Perez, E. J.; Qin, C.; Adachi, C.; Qi, Y. Methylammonium Lead  
846 Bromide Perovskite Light-Emitting Diodes by Chemical Vapor  
847 deposition. *J. Phys. Chem. Lett.* **2017**, *8*, 3193–3198.
- 848 (49) Juarez-Perez, E. J.; Hawash, Z.; Raga, S. R.; Ono, L. K.; Qi, Y.  
849 Thermal Degradation of  $\text{CH}_3\text{NH}_3\text{PbI}_3$  Perovskite into  $\text{NH}_3$  and  $\text{CH}_3\text{I}$   
850 Gases Observed by Coupled Thermogravimetry-Mass Spectrometry  
851 Analysis. *Energy Environ. Sci.* **2016**, *9*, 3406–3410.
- 852 (50) Latini, A.; Gigli, G.; Ciccioli, A. A Study on the Nature of the  
853 Thermal Decomposition of Methylammonium Lead Iodide Perov-  
854 skite  $\text{CH}_3\text{NH}_3\text{PbI}_3$ : An attempt to Rationalise Contradictory  
855 Experimental Results. *Sustainable Energy Fuels* **2017**, *1*, 1351.
- 856 (51) Deretzis, I.; Alberti, A.; Pellegrino, G.; Smecca, E.; Giannazzo,  
857 F.; Sakai, N.; Miyasaka, T.; LaMagna, A. Atomistic Origins of  
858  $\text{CH}_3\text{NH}_3\text{PbI}_3$  degradation to  $\text{PbI}_2$  in vacuum. *Appl. Phys. Lett.* **2015**,  
859 *106*, 131904.
- 860 (52) Stoumpos, C. C.; Malliakas, C. D.; Kanatzidis, M. G.  
861 Semiconducting Tin and Lead Iodide Perovskites with Organic  
862 Cations: Phase Transitions, High Mobilities, and Near-Infrared  
863 Photoluminescent Properties. *Inorg. Chem.* **2013**, *52*, 9019–9038.
- 864 (53) Dimesso, L.; Dimamay, M.; Hamburger, M.; Jaegermann, W.  
865 Properties of  $\text{CH}_3\text{NH}_3\text{PbX}_3$  (X = I, Br, Cl) Powders as Precursors  
866 for Organic/Inorganic Solar Cells. *Chem. Mater.* **2014**, *26*, 6762–  
867 6770.
- 868 (54) Nenon, D. P.; Christians, J. A.; Wheeler, L. M.; Blackburn, J. L.;  
869 Sanehira, E. M.; Dou, B.; Olsen, M. L.; Zhu, K.; Berry, J. J.; Luther, J.  
870 M. Structural and Chemical Evolution of Methylammonium Lead  
871 Halide Perovskites During Thermal Processing from Solution. *Energy*  
872 *Environ. Sci.* **2016**, *9*, 2072–2082.
- 873 (55) Kottokaran, R.; Abbas, H.; Balaji, G.; Zhang, L.; Samiee, M.;  
874 Kitahara, A.; Noack, M.; Dalal, V. Highly Reproducible Vapor  
875 Deposition Technique, Device Physics and Structural Instability of  
876 Perovskite Solar Cells. *IEEE 42nd Photovoltaic Specialist Conference*  
877 *(PVSC)* **2015**, *42*, 1–4.
- 878 (56) Williams, A. E.; Holliman, P. J.; Carnie, M. J.; Davies, M. L.;  
879 Worsley, D. A.; Watson, T. M. Perovskite Processing for Photo-  
880 voltaics: A Spectrothermal Evaluation. *J. Mater. Chem. A* **2014**, *2*,  
881 19338–19346.
- 882 (57) Showman, A. P. Hydrogen Halides on Jupiter and Saturn.  
883 *Icarus* **2001**, *152*, 140–150.
- 884 (58) Jay, A. N.; Daniel, K. A.; Patterson, E. V. Atom-Centered  
885 Density Matrix Propagation Calculations on the Methyl Transfer from  
886  $\text{CH}_3\text{Cl}$  to  $\text{NH}_3$ : Gas-Phase and Continuum-Solvated Trajectories. *J.*  
887 *Chem. Theory Comput.* **2007**, *3*, 336–343.
- (59) Patterson, E. V. Private communication.
- (60) Note that, while the derivation of total pressure from KEML  
889 measurements requires the gas phase composition to be known, 890  
891 assuming the occurrence of processes 8, 9, or 10 has a very small effect  
892 on the calculated pressure, because the relevant average molecular  
893 mass of the vapor phase is very similar in all three cases (see ref 27).  
894 (61) Łubkowski, J.; Błażejowski, J. Thermal Properties and  
895 Thermochemistry of Alkanaminium Bromides. *Thermochim. Acta*  
896 **1990**, *157*, 259–277.
- (62) Dokurno, P.; Łubkowski, J.; Błażejowski, J. Thermal Properties,  
897 Thermolysis and Thermochemistry of Alkanaminium Iodides. 898  
899 *Thermochim. Acta* **1990**, *165*, 31–48.
- (63) Sawicka, M.; Storoniak, P.; Skurski, P.; Błażejowski, J.; Rak, J.  
900 TG-FTIR, DSC and Quantum Chemical Studies of the Thermal  
901 Decomposition of Quaternary Methylammonium Halides. *Chem.*  
902 *Phys.* **2006**, *324*, 425–437.
- (64) Dong, C.; Song, X.; Meijer, E. J.; Chen, G.; Xu, Y.; Yu, J.  
903 Mechanism Studies on Thermal Dissociation of tri-*n*-octylamine  
904 hydrochloride with FTIR, TG, DSC and quantum chemical methods.  
905 *J. Chem. Sci.* **2017**, *129*, 1431–1440.
- (65) <https://www.thermocon.org/>. 907  
908